JOURNAL OF AIRCRAFT
Vol. 36, No. 3, May–June 1999

Fault Tolerance and Extrapolation Stability of a Neural Network Air-Data Estimator

Thomas J. Rohloff* and Ivan Catton†
University of California, Los Angeles, Los Angeles, California 90095

Neural networks have been employed in signal-processing software used to translate the measured pressure distribution from the nose of an aircraft into estimates of freestream static pressure, vehicle speed, and vehicle attitude relative to the flowfield. The performance of the resulting system under normal flight conditions has been previously reported. This paper investigates the performance of the neural network system under more adverse conditions. Specifically, the effect of partial signal failure from the pressure distribution measurements is investigated. Additionally, the stability of the system is tested for applications outside the original domain of the training set. The neural network air-data estimator was found to be both tolerant to faults in the input data and stable when applied to moderate distances of extrapolation.

Nomenclature

C_p = pressure coefficient
M = Mach number
P_i = pressure at port i
P_∞ = freestream static pressure
q_c = dynamic pressure
q_{c2} = dynamic pressure behind the bow shock
α_∞ = freestream angle of attack
β_∞ = freestream angle of sideslip
ε = aerodynamic calibration parameter
θ_i = clock angle for pressure port i
λ_i = flow incidence angle at port i
ϕ_i = cone angle for pressure port i
χ^2 = chi-squared statistical test parameter

Introduction

ACCURATE measurements of air-data parameters are important for both flight testing and control of aircraft. These parameters include the speed and direction of the airmass velocity relative to the aircraft, as well as the freestream static pressure. According to Gracey,[1] air-data measurements are typically performed using intrusive booms that extend beyond the local boundary layer. These booms have been found to be excellent at making steady-state measurements at low to intermediate angles of attack. However, the performance of these instruments deteriorates during high angles of attack and highly dynamic maneuvers. They are also sensitive to vibration and alignment error, and are susceptible to damage during both flight and maintenance.

Flush air-data sensing (FADS) systems, described in Ref. 2, were developed in response to problems associated with intrusive booms. These instruments infer the air-data parameters from pressure measurements taken with an array of ports that are flush to the surface of the aircraft, and are thus completely nonintrusive. However, because the locations of the pressure measurements are on the outer surface of the aircraft, locally induced flowfields can seriously complicate the calibration of these devices. A comprehensive effort to completely characterize an FADS instrument for application on the X-33 single-stage-to-orbit launch vehicle, including extensive wind-tunnel measurements, is described in Ref. 3.

Received July 29, 1998; revision received Oct. 28, 1998; accepted for publication Nov. 24, 1998.

*Graduate Student, Department of Mechanical and Aerospace Engineering, 405 Hilgard Avenue.
†Professor, Department of Mechanical and Aerospace Engineering, 405 Hilgard Avenue.

Development of an FADS interpolation algorithm provides an ideal opportunity for the application of neural network techniques. FADS systems use an input vector composed of 11 pressure measurements P_i to estimate an output vector that includes four air-data parameters (α_∞, β_∞, P_∞, and q_c). The relationship between these two vectors is complex and highly nonlinear. Computational fluid dynamics can be used to study the problem, but the need for a real-time invertible model makes the application of this approach infeasible. Neural networks, which require large quantities of training data, are very well suited to situations such as this, where the more traditional approaches are either insufficient or too complex, but the empirical data are plentiful. These neural network systems allow the correlation of complex nonlinear systems without requiring explicit knowledge of the functional relationship that exists between the input and output variables of the system.

The development of the neural network flush air-data sensing (NNFADS) system was initiated as an alternative to the semi-empirical system described by Whitmore et al.[2] A trained neural network provides a set of explicit calculations, and is therefore insusceptible to the instabilities that were sometimes encountered with the iterative regression techniques described by Whitmore et al. The first successful postflight demonstration of neural network techniques applied to the FADS system was reported in Rohloff and Catton.[4] The FADS air-data estimation was shown to be adequately represented by a trained neural network. However, the data used to train this network only included a single flight profile, and the applicable range of this particular network was limited to similar flight conditions.

The next stage in the development of the NNFADS system, which was reported by Rohloff et al.,[5] used a wider range of flight data pieced together from multiple flight tests to provide a comprehensive training data set across the entire flight envelope of the F-18. Specific techniques were developed for extracting a proper set of neural network training patterns from an overly abundant archive of data. Additionally, the specific techniques used to train the neural networks for this project were reported, including the scheduled adjustments to learning rate parameters during the training process. Two neural networks were trained to estimate static and dynamic pressures across the entire domain on available flight data. The accuracy of these networks was shown to match the accuracy of the semi-empirical system over a wide range of flight conditions from subsonic to supersonic speeds.

The neural networks developed by Rohloff et al.[5] were incorporated into the fault-tolerant NNFADS algorithm described by Rohloff et al.[6] This algorithm was composed of a combination of aerodynamic models and neural network models used to translate a discrete pressure distribution from the nose of an aircraft into a set of air-data parameters including static pressure, dynamic

pressure, Mach number, angle of attack, and angle of sideslip. Techniques were developed to detect and eliminate the effect of a lost signal from the measured pressure distribution. The performance of this system was once again found to match the aerodynamic model-based processor in the estimation of the air-data parameters. The system was also found to be stable, with no major deviations in the air-data estimates, throughout the domain for which it was developed.

The details of the neural network development and the NNFADS algorithm can be found in Refs. 5–7. These references also detail the performance of this system under normal operating conditions. This paper investigates the performance of the NNFADS under more adverse conditions. First, the performance of a new statistical goodness-of-fit test that was developed to identify unacceptable levels of noise in the input measurement, was tested by artificially adding data spikes to the input readings. Second, the stability of the system outside the domain of the training data was studied to ensure that the system would not fail catastrophically under these new conditions.

Current FADS Technology

A prototype real time flush air-data sensing (RT–FADS) system has been developed at the NASA Dryden Flight Research Center.[2] This system was implemented and tested on the NASA F/A-18B Systems Research Aircraft (SRA) over the entire nominal flight envelope of the F-18 from takeoff to landing ($M < 1.6, \alpha_\infty < 50$ deg, -25 deg $< \beta_\infty < +25$ deg). The FADS system was compared with the ship system air-data computer (ADC) measurements, and was shown to be robust to noise in the measured pressures.

The hardware for the RT–FADS system is located in a modified radome of the SRA. The radome and the RT–FADS instrumentation are depicted in Fig. 1. The system consists of the FADS pressure port matrix and the associated measurement transducers. A matrix of 11 pressure orifices was integrated into a composite nosecap and attached in place of the noseboom. The locations of the ports on the nosecap are depicted in Fig. 2, and are defined in terms of clock and cone coordinate angles, ϕ and λ, respectively. The pressures at these locations are sensed by 11 digital absolute pressure transducers located on a palette inside the SRA radome. The transducers are reported by Whitmore et al.[2] to have a repeatability that exceeds 0.01% of full scale with a measurement range from 1.50 to 40.00 psia.

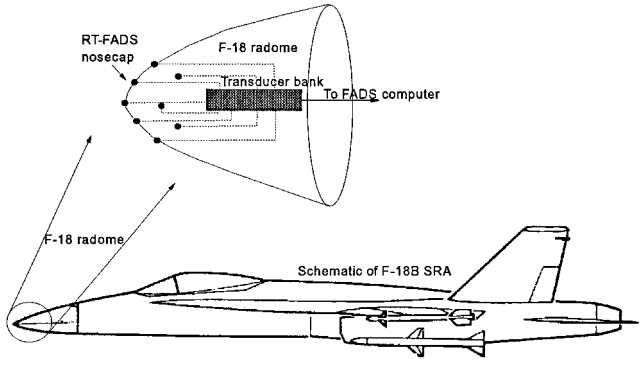

Fig. 1 FADS hardware.

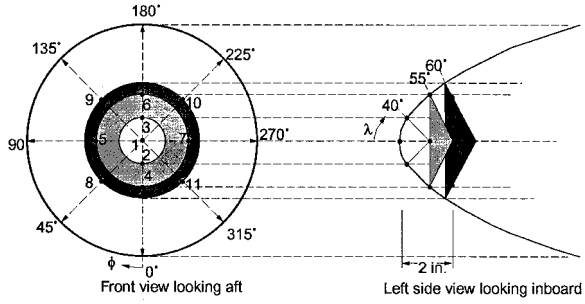

Fig. 2 FADS pressure port configuration.

The reference air-data source reported by Whitmore et al.[2] was generated by combining information from various sources. These measurements included the onboard inertial navigation system attitudes, rates, and accelerations; radar tracking velocity and position data[8]; and rawinsonde weather-balloon sounding data.[9]

The weather-balloon sounding data were verified in-flight by flying 360 deg at a constant speed, and performing a level turn before and after each maneuver. When the indicated airspeed was averaged over the course of the 360-deg turn, the effects of the winds were eliminated. The difference between the averaged airspeed and the averaged radar-derived ground speed was the velocity error for that airspeed caused by the static source error. The velocity error provided an accurate point on the position error curve.

The local wind direction and speed were evaluated by adding this static source velocity error to the indicated airspeed reading and then plotting the ground speed and corrected airspeed as a function of time. Velocity data were converted to Mach numbers using temperature values obtained from the rawindsonde balloon soundings and radar-derived geometric altitude. Local ambient pressure values were evaluated using balloon soundings and radar-derived geometric altitude.

The accuracy of the reference data source techniques was reported in Refs. 2 and 8. The difference between the true and expected values were shown to be $\Delta M < 0.02$, $\Delta\alpha < 0.4$ deg, $\Delta\beta < 0.4$ deg, $\Delta q_c < 12$ psf, and $\Delta P_\infty < 17$ psf. These source data were used for the development of both the RT–FADS model described by Whitmore et al.[2] and the neural network system being investigated in this paper. The accuracy of both models has been shown to be of the same order as the source data for normal flight conditions. A detailed discussion of the accuracy of the neural network model for standard operation can be found in Ref. 7. The focus of this paper is to evaluate the neural network performance under more adverse conditions.

Measurement Redundancy

A major concern during the implementation of this neural-network-based FADS system is its robustness to signal failure. Performance criteria established for this project required that the signal-processing software be robust to the failure of any single lost signal. The preliminary study, discussed in Ref. 4, centered on a single neural network constructed to use all 11 FADS pressure signals in the calculation of the four air-data parameters. Thus, all 11 pressure signals had to be available for this preliminary network to operate properly. A single lost signal caused that initial system to fail. However, it was discovered that neural networks with smaller input layers could also be trained to make the air-data estimates from a reduced set of the FADS pressure signals. More specifically, networks were successfully developed to make air-data estimates from as few as five or six of the pressure signals. This discovery was taken advantage of during the development of a neural-network-based system that is robust to partial signal failure by training several different neural networks with groupings of five or six of the FADS signals each. The estimates from the different pressure groupings can then be averaged to give a best estimate. If any single pressure signal is identified to be corrupted with noise, then any neural net trained with a grouping that includes the failed signal can simply be excluded from the vote. Given that only a limited number of configurations can be reasonably included, it is not possible to guarantee that the system of networks will be able to handle the loss of two or more signals simultaneously, but there will be some combinations of two, three, and even four lost signals that will not affect all of the available networks. The groupings provided in Table 1 were defined using the port index system provided in Fig. 2.

Table 1 Subsets of the FADS array used in NNFADS

Configuration	Port indices
C1	1, 4, 5, 6, 7
C2	2, 3, 8, 9, 10, 11
C3	1, 8, 9, 10, 11
C4	2, 3, 4, 5, 6, 7

Note that each grouping is symmetric about both the vertical and horizontal axes. Furthermore, each configuration includes both points from the center region ($\lambda \leq 40$ deg), and from the outer rings ($\lambda \geq 55$ deg).

Chi-Squared Approach to Signal Filtering

Neural networks trained for the four different configurations provide four estimates for static and dynamic pressures. As was discussed earlier, the four configurations of pressure include two sets of nonoverlapping pairs. Configuration C1 does not have any ports in common with C2, and configuration C3 does not have any ports in common with C4. If any single pressure port returns an inaccurate reading, then two out of the four configuration will still be unaffected. A procedure for identifying estimates that may have been affected by inaccurate pressure measurements is developed next.

It follows from Whitmore et al.,[2] that the relationship between the FADS pressure distribution and the air-data state is, in almost all cases, accurately described by an aerodynamic model in the form

$$P_i = q_{c2}\left(\cos^2\theta_i + \varepsilon \sin^2\theta_i\right) + P_\infty \tag{1}$$

where P_i is the surface pressure at port i; θ_i is the angle between the surface normals at port i and the stagnation point; q_{c2} is the dynamic pressure behind the shock; P_∞ is the freestream static pressure; and ε is a free parameter that is dependent on the air-data state. The form of this model must remain valid, independent of the technique used to determine the air-data parameters. The results from the NNFADS system are no exception. Defining the NNFADS static and dynamic pressure estimates for pressure port configuration j as $\hat{P}_{\infty j}$ and $\hat{q}_{c2j}$, respectively, then the pressure coefficient is given by:

$$\hat{C}_{pij} = \frac{P_i - \hat{P}_{\infty j}}{\hat{q}_{c2j}} = \cos^2\theta_i + \varepsilon_j \sin^2\theta_i \tag{2}$$

Note that both the pressure coefficient C_{pij}, and the free parameter ε_j, are functions of the pressure port configuration being considered. The values θ_i are calculated using the meridian approach developed in Ref. 3. This approach uses pressure differences along the meridians of the FADS sensor ($\phi = 0$, 180 deg or $\phi = 90$, 270 deg) to determine the location of the stagnation point. The local incidence angles θ_i are then calculated relative to the surface normal at the stagnation point. Rearranging Eq. (2):

$$\hat{C}_{pij} - \cos^2\theta_i = \varepsilon_j \sin^2\theta_i \tag{3}$$

Each set of pressure ports for the different configurations j will have a set of equations:

$$\begin{bmatrix} \hat{C}_{plj} - \cos^2\theta_l \\ \vdots \\ \hat{C}_{pnj} - \cos^2\theta_n \end{bmatrix} = \begin{bmatrix} \sin^2\theta_l \\ \vdots \\ \sin^2\theta_n \end{bmatrix} \varepsilon_j \tag{4}$$

The least-squares-error solution for ε_j is obtained by multiplying both sides of Eq. (4) by $\sin^2\theta_i$ and summing over all components:

$$\sum_i \sin^2\theta_i \left(\hat{C}_{pij} - \cos^2\theta_i\right) = \left(\sum_i \sin^4\theta_i\right)\varepsilon_j \tag{5}$$

Solving for ε_j:

$$\varepsilon_j = \frac{\sum_i \sin^2\theta_i \left(\hat{C}_{pij} - \cos^2\theta_i\right)}{\sum_i \sin^4\theta_i} \tag{6}$$

Equation (6) is the least-squares-error solution for ε for pressure port configuration j. A set of FADS pressures associated with the estimated values of the air-data parameters for pressure port configuration j can now be calculated:

$$\hat{P}_{ij} = \hat{q}_{c2j}\left(\cos^2\theta_i + \varepsilon_j \sin^2\theta_i\right) + \hat{P}_{\infty j} \tag{7}$$

The sum of the squares of the residuals between measured and calculated surface pressures is defined as

$$\chi_j^2 = \sum_{i=1}^{n} (\hat{P}_{ij} - P_i)^2 \tag{8}$$

This error measure gives a means of checking for inaccurate FADS pressure readings. If any single reading from the FADS pressure array is inconsistent with the others, then calculated values will no longer correspond to the measured values, and χ_j^2 will consequently increase. The minimum value of χ_j^2 will therefore correspond to the pressure port configuration that is in best agreement with the physical model.

The population distribution of χ_j^2 was calculated for a set of 43,000 frames of flight data, and a histogram was generated in Fig. 3. Based on this analysis, 95% of all the pressure distributions were found to have values of $\chi^2 < 100\,(\text{psf})^2$, and 85% were found to have values of $\chi^2 < 50\,(\text{psf})^2$. During actual applications, using the 85% cutoff [$\chi^2 = 50\,(\text{psf})^2$] was shown to be optimal for signal-filtering

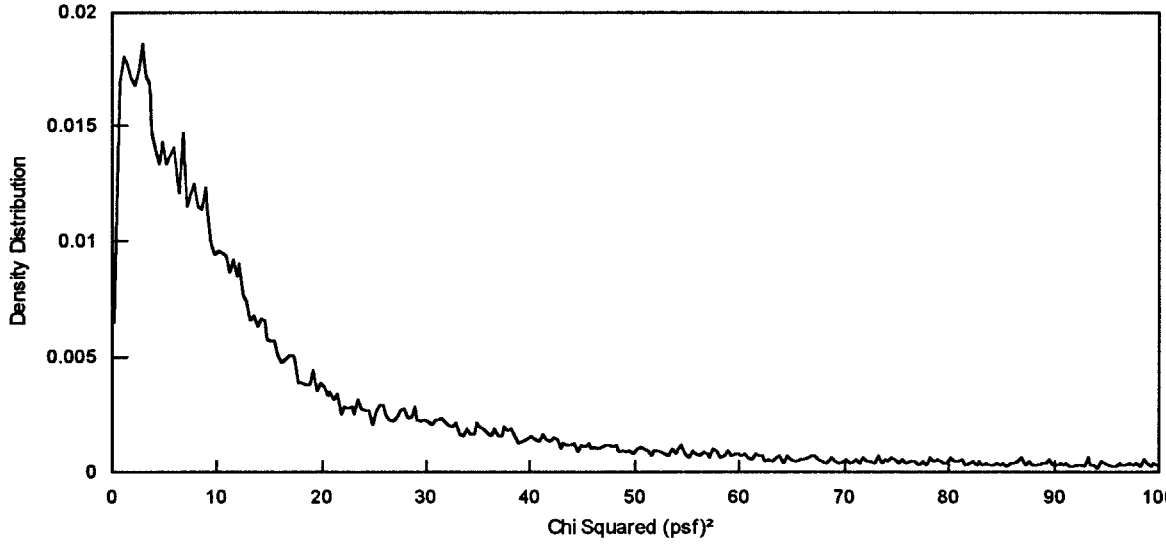

Fig. 3 Chi-squared distribution of NNFADS residuals.

applications. This implies that 15% of the observed pressure distributions are expected to have a higher then acceptable probability of causing errors during the signal processing. If χ_j^2 for all four configurations is below the cutoff value, then all four will be included in the final calculations. If one or more of the χ_j^2 values are over this threshold, then the system pressure readings are considered suspect, and only the configuration with the minimum value of χ_j^2 is used in the final calculations. If all four configurations have χ_j^2 above the threshold, then other techniques will have to be used to define the best estimate.

Robustness of NNFADS to Noise (Biased Input)

The robustness of the NNFADS processor to noise in the input measurements was evaluated by systematically introducing a bias to one or more of the input signals. Flight data were artificially corrupted by adding spikes to the measured signals before they were processed through the NNFADS processor. These tests were performed in two stages. During the first stage only one of the input signals was biased. Measurements from ports 1, 2, 4, 7, and 11 were corrupted one at a time with signal spikes of increasing magnitude. The magnitude of the spikes (ΔP_i) were calculated with

$$\Delta P_i = \pm \text{NSR} \times \bar{P}_i$$

where $\bar{P}_i$ is the average of the input signals, and NSR is the noise-to-signal ratio that was varied from 0 to 0.5. During the second stage of this test, two ports were corrupted at a time. Port 1 was consistently biased with NSR $= +0.2$, and ports 2, 4, 7, and 11 were corrupted one at a time with spikes ranging from NSR $= 0.0$ to ± 0.5.

The percent rms error in the estimates of P_∞ and q_c with one biased input signal were plotted in Figs. 4 and 5 as a function of the NSR. Each of the graphs includes two curves. The first curve was generated without any fault detection, and the second was created with a system that included the χ^2 fault-detection techniques. Without the filter, the neural network estimates of both parameters steadily degraded as the noise level was increased. However, with the fault-detection routine activated, the neural network system performed dramatically better, and was found to be only marginally affected by the spike in the input signal. As the NSR increased from 0 to 0.35, the χ^2 filter most often identified the artificial data spike. At NSR $= 0.2$, the error in P_∞ was $\sim 3\%$, and the error in q_c was just over 5%. Between NSR $= 0.2$ and 0.35, the error in both of these estimates decreased to the same value as at NSR $= 0.0$. The effect of data bias in any single signal was always identified for NSR > 0.35.

The percent rms error in the estimates of P_∞ and q_c with two biased input signals were plotted in Figs. 6 and 7. The magnitude of the error increased significantly over one biased port, even with the signal classifier activated. The fault-detection algorithm does manage to reduce the average level of error if the two failed ports leave at least one unaffected input configuration. Otherwise, the best estimate of the air data will be corrupted by at least one bad signal.

The NNFADS system is robust to any level of noise in any one pressure port. The criteria for this project have therefore been met. If future systems require a higher level of fault tolerance, then the techniques applied in this system can easily be adapted. Additional independent sets of FADS pressure ports can be used to increase the robustness of the system. For example, if three independent sets were available, then the system would be resistant to the loss of any two signals.

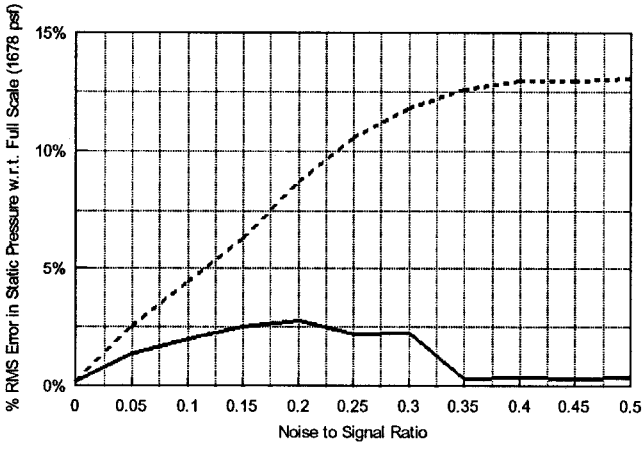

Fig. 4 Single port bias—static pressure: - - - -, fault detection off, and ——, fault detection on.

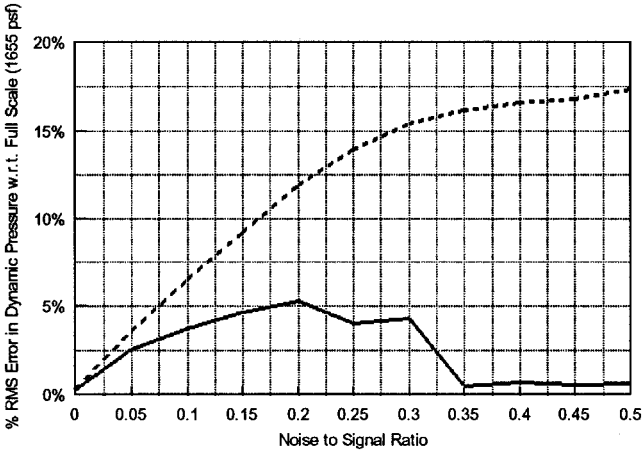

Fig. 5 Single port bias—dynamic pressure: - - - -, fault detection off, and ——, fault detection on.

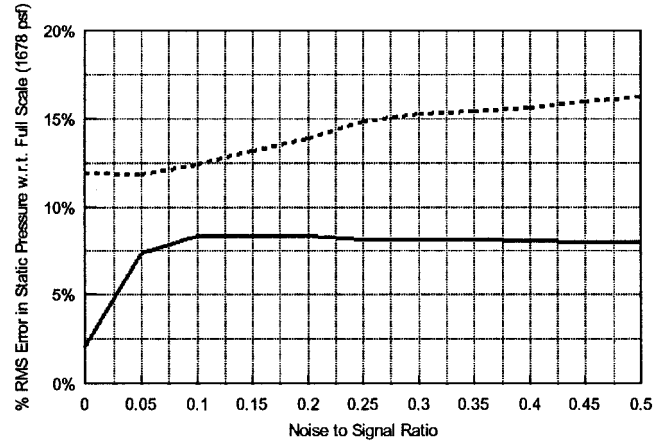

Fig. 6 Double port bias—static pressure: - - - -, fault detection off, and ——, fault detection on.

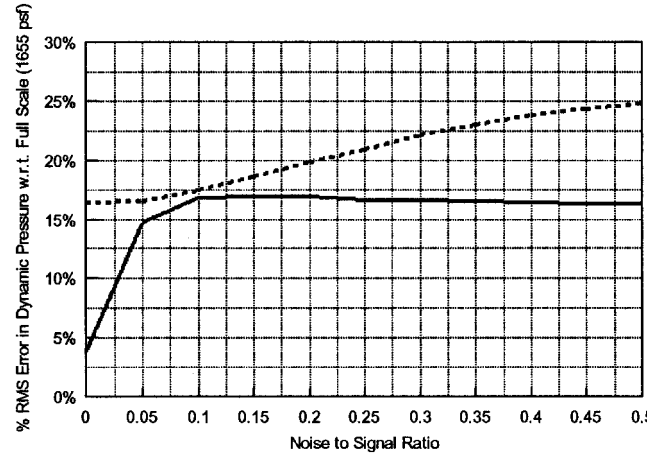

Fig. 7 Double port bias—dynamic pressure: - - - -, fault detection off, and ——, fault detection on.

The calculations of the angles of attack and sideslip do not require that the pressure measurements be processed directly with a neural network.[6] Instead, the meridian approach, discussed in Ref. 3, is used to estimate a local value of the incidence angles. The freestream values are then just a function of these local values and the Mach number. The process used to make these estimates facilitates the elimination of the effect of failed inputs without the use of the chi-squared filter.

Total Extrapolation Distance Outside the Training Domain

Data generated with an inverted version of the RT–FADS system, described in Ref. 2, were used to test the extrapolation capabilities of the NNFADS system. The exteriority, defined in Ref. 10, was used as a measure of the distance of any point outside the domain of the archived flight data to the convex hull polytope of the training set. Convex hulls are multidimensional surfaces that tightly encompass a set of multidimensional data. The method presented in Ref. 10 uses standard mathematical procedures to determine the vertices of the convex hull of the training data used to construct a neural network. Once this surface is defined, the Euclidean distance of a new point to that surface can be calculated. This distance, termed the exteriority, is defined as zero if the point lies on or within the convex hull, and it is positive if it lies outside. The exteriority is therefore a measure of the distance between a new point and the domain of the original training set. The reader is referred to Refs. 5 and 7 for a more complete discussion of convex hulls and exteriority.

The convex hull polytope encompassing the four-dimensional volume in the air-data space was assumed to be a good representation of the limits of the available data. It is important to note that the air-data vectors used to define the location within the air-data space had to be normalized between 0 and 1. This ensured that the scale of the exteriority would be the same in any direction. Furthermore, the normalized exteriority represents the percent distance outside the training set relative to the full scale values of the air-data parameters.

To test the extrapolation capabilities of the air-data neural networks, the signal-filtering techniques were not employed during these trials. The normalized standard deviation is given as a function of exteriority in Fig. 8. The deviation of all four air-data parameters stay within 10% rms error for extrapolation distances as high as 20%. Above 20% exteriorities, the error in the incidence angles increased to a range of 15–20%. The accuracy of both M and P_∞ stay within 10% for the entire range of extrapolation distances being considered. This demonstrates that the processor does not fail catastrophically outside the domain of the training set.

The data used in this test were generated with the inverted RT–FADS algorithm. However, the RT–FADS system was calibrated on the same data set used to train the neural networks of the NNFADS system. This means that when the data set was generated for these tests, the RT–FADS system was also extrapolating outside its original domain of validity. Therefore, it is not clear whether the error observed in Fig. 8 was a result of the NNFADS system or of the generated data set. However, it is not plausible to assume that the error associated with extrapolation would be the same for both systems. Thus, for extrapolation distances of less than 20%, the stability of both the NNFADS system and the RT–FADS system is validated.

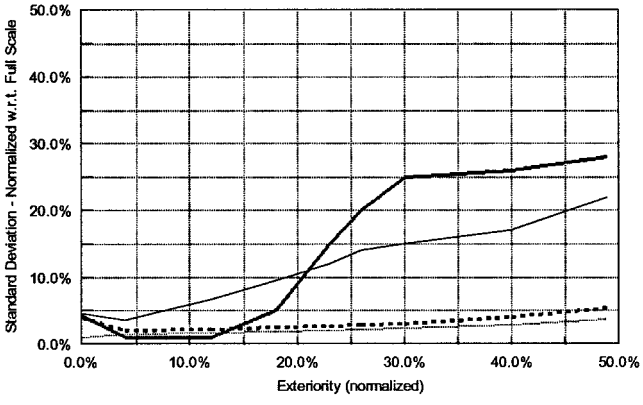

Fig. 8 Extrapolation outside the training set: ——, angle of attack; ——, angle of side slip; - - - -, Mach number; and ·····, static pressure.

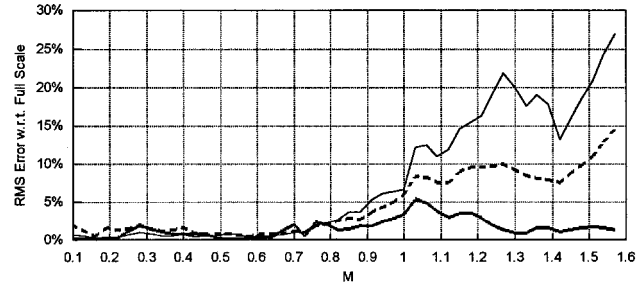

Fig. 9 Extrapolation tests using flight data. Neural network trained for $0.1 < M < 0.75$: ——, static pressure; ——, dynamic pressure; and - - - -, Mach number.

Extrapolation Within the Training Domain in Direction of Mach Number

A second extrapolation test was performed with the NNFADS system. In this trial, a version of the NNFADS system was constructed with neural networks trained only with the subsonic flight data ($M < 0.75$). This system was subsequently applied to a set of test data covering the entire envelope of the flight data, including $M > 0.75$. A graph of the rms error of the air-data parameters as a function of Mach number is provided in Fig. 9. As can be seen from the graph, the estimates for P_∞ and q_{c2} degrade by several percent through the transonic region. Despite the fact that the neural network used in this test was not trained for supersonic conditions, the accuracy of the estimates for static pressure appears to be only slightly affected through the larger Mach numbers. However, the rms errors for both q_{c2} and M continue to degrade as M increases into the supersonic regime. The deterioration is a smooth increasing function of the distance outside the domain of the training set. This reaffirms the results of the previous section. The neural network processors do not fail catastrophically, and can be applied a moderate distance outside the original domain of the training set.

The two incidence angles are unaffected by this test. The correlations for translating between local and freestream values were not dependent on the value of the Mach number, and the estimates of α and β were not included in Fig. 9.

Conclusions

The neural network air-data estimator was shown to be tolerant to both partial and complete failure of any single measurement out of the 11 pressure readings. Redundant subsets of the array of measurements were used in conjunction with a statistical goodness-of-fit test to identify and eliminate the effect of a signal that was inconsistent with the current flight conditions. This same technique can easily be adapted in the development of systems that are tolerant to two or more signal failures.

The neural network system was also demonstrated to be stable when applied to new points outside the original domain of the training data. The extrapolation capabilities of the system were tested with both physical models and actual flight data.

Based on the results of both the previous and current studies, neural network techniques can be successfully employed for the signal processing needs of flush air-data sensing systems. The resulting system can be both accurate under nominal operating conditions, and robust under more adverse conditions. Neural network techniques can therefore be used as an alternative to the methods currently being employed for air-data signal processing.

Acknowledgments

This work was supported under Grant NCC 2-374 from NASA Dryden Flight Research Center, Edwards Air Force Base, California.

We thank S. A. Whitmore, this work would not have been possible without his support and guidance.

References

[1]Gracey, W., "Measurement of Aircraft Speed and Altitude," NASA RP 1046, May 1980.

[2]Whitmore, S. A., Davis, R. J., and Fife, J. M., "In-Flight Demonstration of a Real-Time Flush Airdata Sensing (RT-FADS) System," NASA TM 104314, Oct. 1995.

[3]Whitmore, S. A., Cobleigh, B. R., and Haering, E. A., "Architecture, Algorithms, and Calibration of the X-33 Flush Airdata Sensing (FADS) System," AIAA Paper 98-0201, Jan. 1998.

[4]Rohloff, T. J., and Catton, I., "Development of a Neural Network Flush Airdata Sensing System," *Proceedings of the 1996 ASME International Mechanical Engineering Congress and Exposition*, FED-Vol. 242, American Society of Mechanical Engineers, Fairfield, NJ, 1996, pp. 39–43.

[5]Rohloff, T. J., Whitmore, S. A., and Catton, I., "Air Data Sensing from Surface Pressure Measurements Using a Neural Network Method," *AIAA Journal*, Vol. 36, No. 11, 1998, pp. 2094–2101.

[6]Rohloff, T. J., Whitmore, S. A., and Catton, I., "A Fault Tolerant Neural Network Algorithm for Flush Air Data Sensing," *Journal of Aircraft* (to be published).

[7]Rohloff, T. J., "Development and Evaluation of Neural Network Flush Air Data Sensing Systems," Ph.D. Dissertation, Dept. of Mechanical and Aerospace Engineering, Univ. of California, Los Angeles, CA, 1998.

[8]Haering, E. A., Jr., and Whitmore, S. A., "FORTRAN Program for Analyzing Ground-Based Radar Data: Usage and Derivations, Version 6.2," NASA TP-3430, 1994.

[9]Ehernberger, L. J., Haering, E. A., Jr., Lockhart, M. G., and Teets, E. H., "Atmospheric Analysis for Airdata Calibration on Research Aircraft," AIAA Paper 92-0293, Jan. 1992.

[10]Courrieu, P., "Three Algorithms for Estimating the Domain of Validity of Feedforward Neural Networks," *Neural Networks*, Vol. 7, No. 1, 1994, pp. 169–174.